

Profiles in Volume Phase Holograms in Cp_2TiCl_2 : PMMA

T. Lückemeyer and H. Franke

FB Physik, Universität, Postfach 4469, D-4500 Osnabrück, Fed. Rep. Germany

Received 23 November 1987/Accepted 2 February 1988

Abstract. A method for measuring depth profiles in volume phase gratings recorded in doped poly-(methyl methacrylate) (PMMA) is demonstrated. The profiles are the product of photosensitivity and light distribution. Photosensitivity is governed by the distribution of residual monomer. Insensitive PMMA samples may be sensitized by in-diffusion of monomer. The photoinitiator bis(cyclopentadienyl)-titanium-dichloride (Cp_2TiCl_2) is found to be moisture sensitive.

PACS: 42.40, 82.35

The use of photosensitive Poly-(methyl methacrylate) (PMMA) as a material for optical storage has been investigated by several researchers [1–3]. The photochemical mechanism of the formation of the refractive index pattern is due to photopolymerisation of residual monomer. The light-intensity pattern acting on the photoinitiator molecules causes a pattern of radicals. These radicals initiate the polymerisation of the residual monomer in the exposed regions. Thus a refractive-index pattern is formed due to the light intensity distribution [4].

The photorefractive system we use here consists of the polymer matrix PMMA, the residual monomer and the photoinitiator bis(cyclopentadienyl)-titanium-dichloride (Cp_2TiCl_2). This organometallic compound is sensitive in the green spectral region (e.g., 514.5 nm Ar laser). The photochemical reaction has been reported in the literature [5, 6], and the system has been investigated as a material for holographic storage [7, 8]. Recording of volume phase holograms in photosensitized material is usually performed with open samples. That means, all kinds of diffusion may occur between sample preparation and recording of the hologram, e.g. monomer out-diffusion, oxygen in-diffusion, moisture pickup etc. All these diffusion processes may cause profiles of the photosensitivity. The purpose of this paper is to find out the role of the different diffusion processes. We want to demonstrate a method of measuring actual profiles in volume phase

gratings. Being able to measure actual profiles the next step is to find out the influence of different diffusion processes on the photosensitivity. Finally the chance of designing special volume phase holograms appears attractive.

1. Experimental

The preparation of the photosensitive PMMA samples is described elsewhere [7].

1.1. Recording of Volume Phase Gratings

A light intensity grating is formed by a two-wave interference pattern using a usual two-beam holographic set-up, as described in [9]. The two expanded beams of an Ar laser (514.5 nm) interfere symmetrically at the sample, forming a light pattern

$$I(x) = I_0[1 + m \cos(kx)]. \quad (1)$$

$I_0 = I_R + I_S$ is the entire intensity of the reference beam (I_R) and the signal beam (I_S). For $I_R = I_S$ the modulation index m is $m = 1$ and (1) may be rewritten:

$$I(x) = I_0[1 + \cos(kx)]. \quad (1')$$

The intensity changes periodically between $I(x) = I_0$ and $I(x) = 0$ with the spatial frequency $k = 2\pi/\Lambda$. The grating constant Λ is determined by the angle between

the interfering beams (2Θ) and the wavelength of the recording light according to

$$A = \lambda/2 \sin \Theta. \quad (2)$$

A linear photorefractive response to the intensity grating (1') leads to a refractive-index grating:

$$n(x) = n_0 + \Delta n(1 + \cos kx)/2. \quad (3)$$

The growth curves or the formation of the grating with exposure time have been studied in [7,8] for our photorefractive system. For the study of profiles we must avoid saturation effects and therefore we stop the exposure after 5 min, which is in the linear region of the growth curve Δn versus time [8].

1.2. Measurement of Profiles $\Delta n(z)$

Generally the recorded volume phase gratings may exhibit profiles in the z direction (Fig. 1). This means that Δn is not constant as a function of z . The position of such a grating with depth profile in the sample is illustrated in Fig. 1. The grating constant of $6 \mu\text{m}$ is a typical value for our investigated patterns. The occurrence of such profiles in PMMA has been reported by Moran et al. [9].

For constant values of Δn and negligible absorption effects (no absorption grating) the diffraction efficiency η of such grating is given by the Kogelnik formula [10, 11]:

$$\eta(z) = \sin^2 \left[\frac{\pi}{2\lambda \cos \Theta} \Delta n(z) dz \right] \cdot \exp \left(\frac{-2\alpha dz}{\cos \Theta} \right) \quad (4)$$

with dz : sample thickness Θ : Bragg angle, and α : absorption constant. Our photosensitive system exhibits absorption in the green spectral region [8]. Measuring the diffraction efficiency with a HeNe laser beam ($\lambda = 633 \text{ nm}$), we can neglect the absorption part

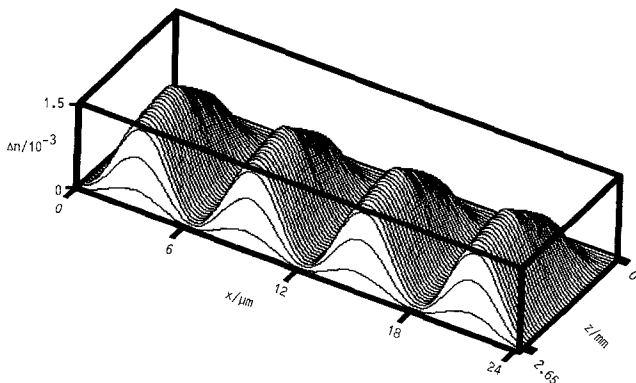


Fig. 1. Volume phase grating with a profile $\Delta n(z)$ in the PMMA sample

in (4).

$$\eta(z) = \sin^2 \left[\frac{\pi}{2\lambda \cos \Theta} \Delta n(z) dz \right], \quad (4')$$

on the other hand, we use the definition of the experimental diffraction efficiency

$$\eta = I_D / (I_D + I_T) \quad (5)$$

with I_D : intensity of the diffracted beam, and I_T : intensity of the transmitted beam. This definition may lead to values of η close to 100%.

For a slowly varying $\Delta n(z)$ the Kogelnik formula (4) has to be rewritten to [12]:

$$\eta(z) = \sin^2 \left[\frac{\pi}{2\lambda \cos \Theta} \int_0^z \Delta n(z') dz' \right]. \quad (6)$$

Again the absorption part is neglected and $\eta(z)$ is compatible with the definition according to (5).

Figure 2 shows the experimental set-up for the measurement of $\eta(z)$. The central part is a microtome of the type "autocut 2050" (Fa. Reichert). Thin ($1-10 \mu\text{m}$) slices of the volume phase grating are cut off the PMMA block and the remaining diffraction efficiency is recorded. The sample remains mounted in order to keep the sample in the same position and orientation after each cut. There is a minimum remaining block thickness of about 0.2 mm , when no more cuts can be performed because of mechanical problems. Thus PMMA blocks with volume phase gratings can be measured between their original thickness of $1-3 \text{ mm}$ down to 0.2 mm with respect to their diffraction efficiency $\eta(z)$.

In order to determine $\Delta n(z)$ from the measured values of $\eta(z)$ Eq. (6) has to be solved. Usually we have more than one period $\eta(z)$, oscillating between 0 and 100%. The measured values $\eta(z)$ have to be transfor-

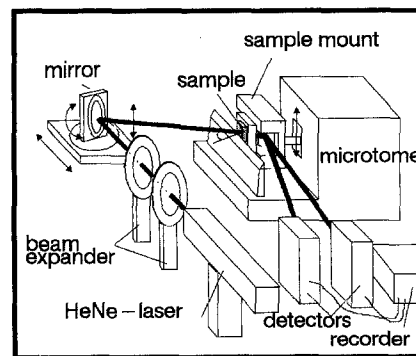


Fig. 2. Experimental set up for measuring the diffraction efficiency of a volume phase grating as a function of thickness $\eta = \eta(z)$

med into a monotonous set according to

$$H(z_i) = (-1)^{n+1} \cdot \arcsin \sqrt{\eta(z_i)} + \text{Int} \left\{ \frac{n}{2} \right\} \cdot \pi \quad (7)$$

with n denoting the extrema of $\eta(z_i)$ and $\text{Int}\{x\}$ being the integer function. After smoothing the experimental values (spline function) (6) can be solved to

$$\Delta n(z) = (2 \cdot \lambda \cdot \cos \Theta / \pi) \cdot \frac{\partial}{\partial z} \text{SPLINE} \{H(z_i)\}. \quad (8)$$

The smoothing of the values $H(z_i)$ is done within the experimental error of $\eta(z)$ or $H(z_i)$.

1.3. Measurement of Absorption Profiles $\alpha(z)$

The photosensitive-doped PMMA samples should be homogenous after preparation, including the photoinitiator distribution. However, any chemical reaction of the dye molecules with in-diffused oxygen or moisture may cause a chemical reaction leading to bleaching of the photoinitiator. In these regions the photosensitivity of the samples is reduced due to destroyed initiator molecules. Thus the measurement of the absorption constant for the recording light is another necessary step to achieve the full information about the photosensitive profile of the samples.

The absorbed intensity of a thin slice dz of the sample is given by

$$dI = -\alpha(z) dz \cdot I \quad (9)$$

with the absorption constant $\alpha(z)$. Integration of (8) leads to

$$I(z) = I(0) \cdot \exp \left(-\int_0^z \alpha(z') dz' \right). \quad (10)$$

In a conventional spectrometer (e.g., Cary 17D) the optical density $D(z) = \log(I(0)/I(z))$ of a sample with thickness z is measured. By combining the set-up, illustrated in Fig. 2, with a conventional spectrometer we are able to measure the absorption profile of a sample

$$\alpha(z) = [dD(z)/dz] \log e. \quad (11)$$

Therefore the sample mount from the microtome is placed in the spectrometer and between cutting off the thin slices the absorption at $\lambda = 514 \text{ nm}$ is recorded.

1.4. Diffusion Experiments

For storage in controlled atmosphere (N_2, O_2) and diffusion experiments we use the set-up, illustrated in Fig. 3. This chamber is suitable for vacuum treatment, and out- or in-diffusion experiments. The diffusion experiments with MMA monomer were performed at

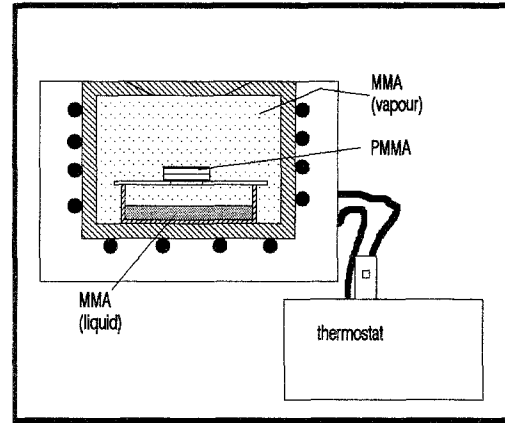


Fig. 3. Experimental set-up for storage in controlled atmosphere and diffusion experiments

$T = 90^\circ\text{C}$. In-diffusion at lower temperatures is not possible with PMMA at saturation vapor pressures of MMA because of cracks at the surfaces of the sample. At 90°C the saturation partial vapor pressure of MMA is 70500 Pa (0.7 atm) and the surfaces remain smooth.

2. Experimental Results

Before looking into special $\Delta n(z)$ profiles we have checked our method performing 2 experiments.

1) A grating is recorded in a sample passing the $\eta = 100\%$ value with a saturation diffraction efficiency of 35%. This block measured in the set-up illustrated in Fig. 2. Now, as a function of thickness the $\eta(z)$ starts at $\eta(d) = 35\%$ passes $\eta(d/2) = 100\%$ and decreases to zero. Thus the recording curve is "reconstructed".

2) In a second experiment a grating with a relative large surface of 1 cm^2 is cut in the y direction (Fig. 1). The sample a is cut starting at the top surface ($z = 0$) and the sample b is cut starting at the back surface ($z = d$). The resulting profiles coincide in their reflected images.

The self consistency of the method can be seen from Fig. 4. The experimental values are plotted and the solid line represents the calculated of $\eta(z)$ from the $\Delta n(z)$ profile according to (6).

2.1. Profiles for Different Recording Intensities

First we want to check how the recording intensity influences the obtained $\Delta n(z)$ profile of the same photosensitive samples. Two pieces are prepared out of the same polymer block. Within 2 h after taking out of the preparation cell the grating is recorded with different intensities during 5 min of exposure. In this period of time we are in the region of linear growth ($\Delta n/t$) with exposure time. This linear growth is

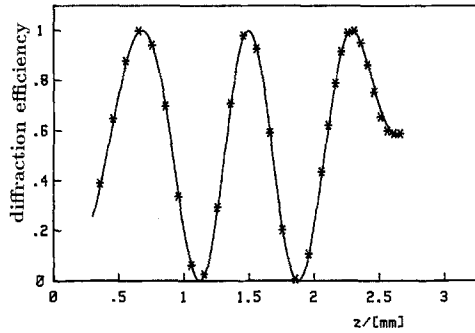


Fig. 4. Diffraction efficiency as a function of sample thickness z , measured with the set-up of Fig. 2. Parameters: sample thickness $d=2.66$ mm, recording intensity $I=478$ mW/cm² for 5 min, grating constant $\Lambda=6$ μ m

reported to be proportional to the recording intensity [8]. This result is obtained neglecting any $\Delta n(z)$ profile, so it has to be transformed into $\Delta n/t \sim I$ with Δn representing the average refractive index amplitude. From Fig. 5 can be seen that the profiles $\Delta n(z)$ are similar for different recording intensities. The amplitude and the maximum value are proportional to the recording intensity. Thus in this linear region of the growth curve the linear response of the change in refractive index with exposed energy is a good approximation.

$$\Delta n/t = c \cdot I = c \cdot w/t \Rightarrow \Delta n = c \cdot w \quad (12)$$

with c : const, I : recording energy and t : recording time.

2.2. Profiles due to Sample Aging

From early experiences [6], we know that leaving photosensitive samples for a few weeks under normal conditions leads to less sensitive samples. In order to get more information about the mechanism of the decreasing sensitivity we record gratings with the same recording parameters in samples of different age. The compared samples are prepared from the same polymer block. In Fig. 6 is illustrated how the $\Delta n(z)$ profiles get smoother with aging time and how they get restricted to the inner part of the samples. From Fig. 6 we can understand why our samples become insensitive after an aging period of, e.g., 3 months. The profile shown in Fig. 6 is obtained by cutting the sample from the front surface, which means the surface facing the light pattern in the recording procedure. The details of the profiles close to the front surface are shown in Fig. 7. Recording the grating 1 h after mounting the fresh sample from the cell leads to an intensive zone of 10 μ m below the surface. After 89 h this zone has reached a depth of 140 μ m.

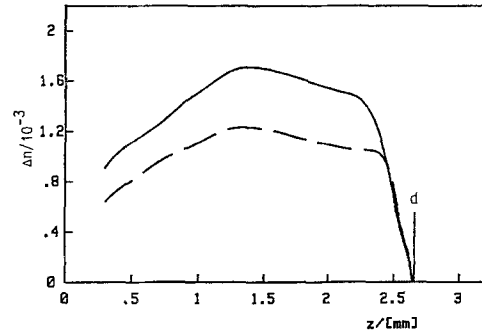


Fig. 5. $\Delta n(z)$ profiles of volume phase gratings recorded with different intensities. — $I=478$ mW/cm², the corresponding $\eta(z)$ curve is shown in Fig. 4. - - - $I=354$ mW/cm². Recording time is 5 min $\Lambda=6$ μ m

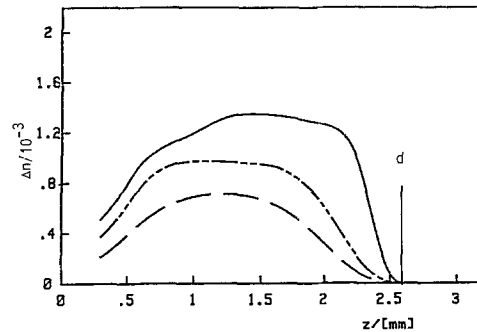


Fig. 6. Depth profiles of volume phase gratings in samples which have been stored for some time (t_s) between preparation and recording of the grating. Storage is done under normal conditions, at room temperature, in air — $t_s=4$ days, - - - $t_s=21$ days, - · - $t_s=42$ days. Recording intensity is 460 mW/cm² for 5 min

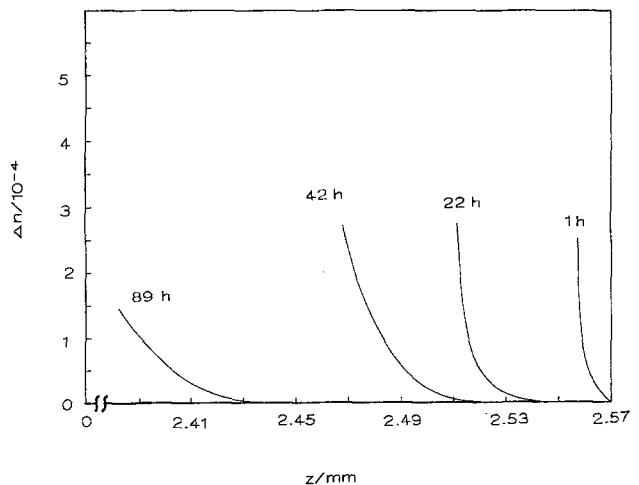


Fig. 7. Depth profiles of volume phase gratings at the surface of aged samples. The PMMA samples were cut from the front surface. Storage times are indicated. Recording intensity is 280 mW/cm² for 5 min, $\Lambda=6$ μ m

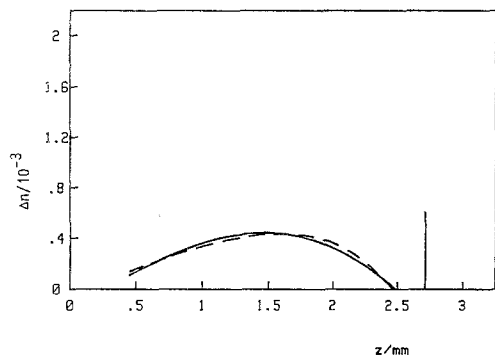


Fig. 8. Depth profiles of gratings 2 samples aged for 112 h at 50°C — in N_2 atmosphere, or - - - in air

Influence of Oxygen. Molecular oxygen is known to react with radicals, MMA – or photoinitiated radicals [13], leading to long living radicals decreasing the residual polymerisation kinetics. In Fig. 8 we compare the volume phase gratings recorded into 2 samples which are the same except for the fact that one has been aged at 50°C for 112 h in N_2 atmosphere and the other one has been aged in air with the usual oxygen content. Both profiles coincide within the experimental error. There is obviously no significant change in the photosensitivity due to aging in an O_2 -free atmosphere.

2.3. Profiles by in-Diffusion of Monomer

If the loss of photosensitivity during aging of our samples is due to monomer out-diffusion, one should be able to restore the sensitivity by in-diffusion of MMA monomer. These experiments can be done with PMMA samples containing the photoinitiator Cp_2TiCl_2 but being free of residual monomer. Samples of this type may be prepared by heating for 3 h at 90°C. They are completely insensitive. No detectable grating can be recorded even at high exposure levels.

In the diffusion cell, illustrated in Fig. 3, MMA monomer can be diffused back into the Cp_2TiCl_2 :PMMA samples at 90°C. After this diffusion process the samples are sensitive again and holographic gratings may be recorded. In Fig. 9 examples of samples, with different in-diffusion periods are shown. The exposure parameters and all other procedures were the same for these samples. With increasing diffusion time the maximum value of $\Delta n(z)$ is increasing and the profile is shifted towards the middle of the sample. Interesting is the almost constant insensitive region of 140 μm below the surface.

Another interesting experiment is shown in Fig. 10. Here the MMA monomer has been in-diffused from the front and from the back surface as well. This sample

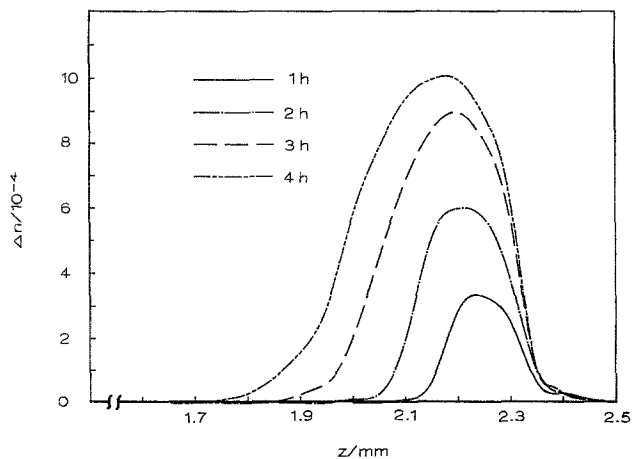


Fig. 9. Depth profiles of gratings in MMA in-diffused samples for different diffusion periods. Diffusion is performed at 90°C, exposure is done with $I = 280 \text{ mW/cm}^2$ for 5 min

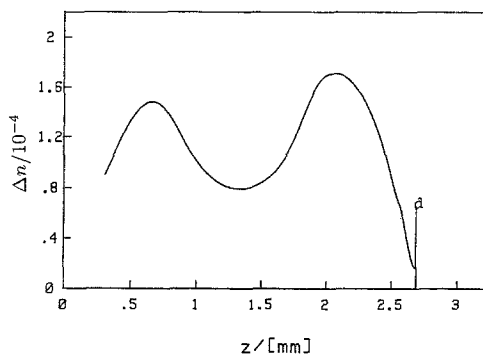


Fig. 10. Depth profile of a grating in a sample with MMA in-diffused from the front and from the back surface. Diffusion time is 4 h, exposure is done with $I = 275 \text{ mW/cm}^2$ for 5 min

was in-diffused for 4 h, but it has not been completely insensitive before. The heating period has only been 30 min. Thus the relative complicated overlap 3 profiles of sensitivity occurs: in-diffused from front surface, in-diffused from back surface and residual MMA content in the middle. The maximum in the $\Delta n(z)$ profile next to the back surface is lower than that close to the front surface. This is obviously due to the light absorption in the recording process.

2.4. Absorption Profiles due to Photoinitiator Reaction

So far we have neglected any influence of the photoinitiator bis(cyclopentadienyl)-titanium-dichloride (Cp_2TiCl_2) on the profiles of photosensitivity. A first hint on a contribution in the surface region is given in Fig. 9. Here the insensitivity of the 140 μm deep surface region should not be due to lack of monomer. Cp_2TiCl_2 turns out to react with H_2O . In Fig. 11 the

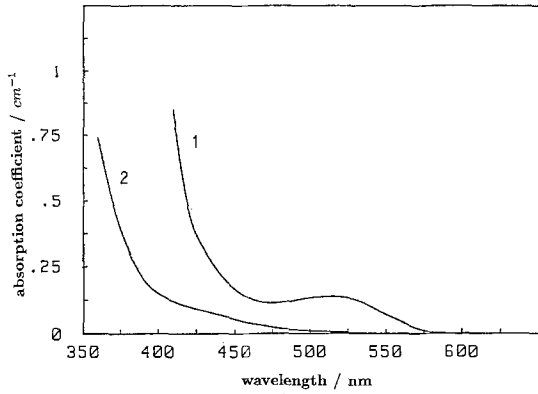


Fig. 11. Absorption spectra of the photoinitiator; curve 1: Cp_2TiCl_2 as prepared; curve 2: Cp_2TiCl_2 after reaction with H_2O

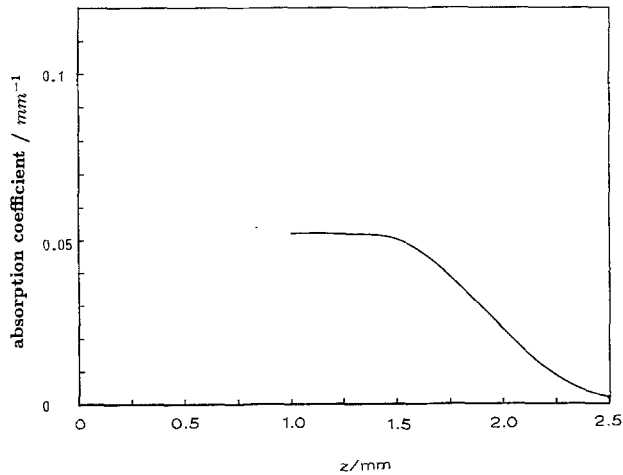


Fig. 12. Absorption profile of a Cp_2TiCl_2 :PMMA sample after 24 h storage in distilled water at room temperature

absorption spectra of the photoinitiator before and after reaction with H_2O are plotted. The spectra are measured with a solution of the material (25 mg/dm^3) in MMA. From spectrum 2 in Fig. 11 we can see that the reaction with water destroys the photoinitiator. This process may happen in our photosensitive PMMA samples as well.

As described in Sect. 1.3, we measure the absorption profile of a photosensitive block after storage for 24 h in distilled water. The result is shown in Fig. 12. The absorption constant is zero at the surface and within a zone of 1 mm depth it reaches the original value. The $\Delta n(z)$ profile of a grating recorded in a sample after storage for 24 h at 50°C is shown in Fig. 13. The insensitive zone has increased to a depth of 0.6 mm.

The storage in H_2O is an extreme case, realistic is the storage in normal humid atmosphere and because we have not excluded moisture in our storage at-

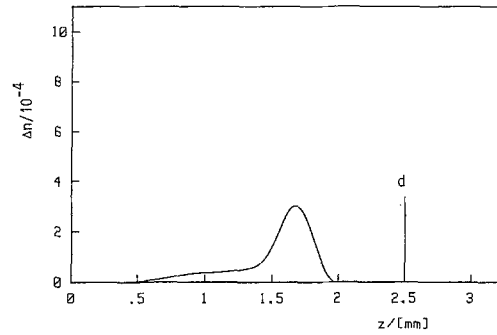


Fig. 13. Depth profile of a grating recorded in a Cp_2TiCl_2 :PMMA sample after storage in H_2O for 24 h at 50°C

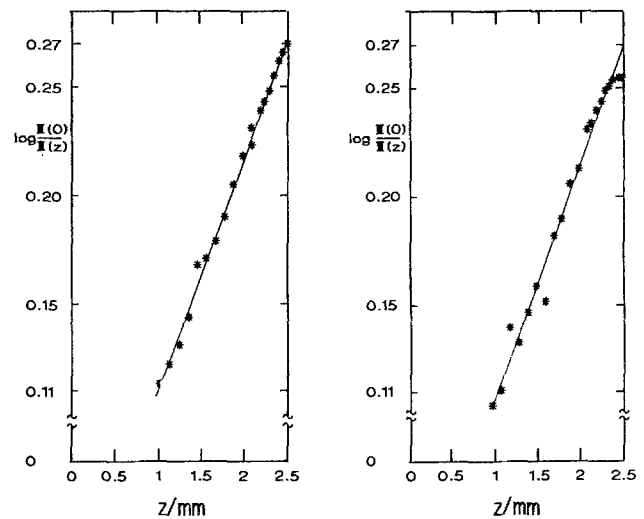


Fig. 14a, b. Optical density $D(z)$ at $\lambda = 514 \text{ nm}$ for a Cp_2TiCl_2 :PMMA sample (a) sample as prepared; (b) after aging for 3 h at 90°C in a standing N_2 atmosphere

mospheres with special care we have to consider the influence of residual moisture upon profiles near the surface. In Fig. 14 the optical density of a fresh sample (Fig. 14a) and a sample after insensitivity treatment at 3 h at 90°C in standing N_2 atmosphere is compared. The fresh sample exhibits a nice and constant $\alpha(z)$ profile, while there is an influence in case of the heat treated sample at the surface region due to residual moisture (Fig. 14b).

3. Discussion

The mechanism of increasing refractive index in our photosensitive Cp_2TiCl_2 :PMMA samples is the photopolymerisation of residual monomer. In the region of short exposure times, that is the linear region of the growth curve $\Delta n(t)$ the radical distribution is approximately linear to the intensity pattern [8]. Our

results for different recording intensities indicate that the experimental result for $\Delta n = c \cdot I \cdot t$ with $c = \text{const}$ may be generalized for the profile $\Delta n(z)$.

3.1. Monomer Distribution

The profiles of the volume phase gratings $\Delta n(z)$ recorded in aged samples may be interpreted as being due to

- a) monomer out-diffusion or
- b) in-diffusion of the inhibitor O_2 .

However from further results we would decide for the monomer distribution being the main source for the observed profiles in photosensitivity

– long time annealing in O_2 or in N_2 atmosphere does not show a significant influence upon the achieved $\Delta n(z)$ profiles (Fig. 8).

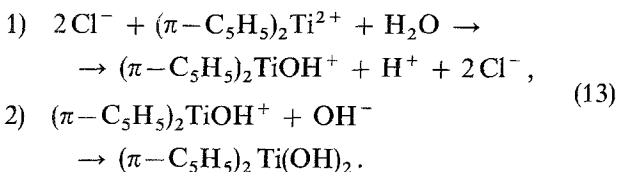
– After an annealing treatment of 3 h at 90°C the samples are completely insensitive. By consequent in-diffusion of monomer they become sensitive again. The maximum $\Delta n(z)$ values are comparable with fresh samples (10^{-3} in Fig. 9), although these samples should be saturated with oxygen after 3 h annealing in air.

The undetected influence of oxygen on the $\Delta n(z)$ profiles does not indicate that there is no oxygen involved. The lowering of polymerisation kinetics may be compensated by increasing the molar refraction due to copolymerisation with $-\text{O}-\text{O}-$.

On the other hand, especially the reconstruction of photosensitivity by indiffusion of monomer gives strong evidence for the monomer concentration dominating the photosensitivity. Measurement of the $\Delta n(z)$ profiles as a function of diffusion time may be used to determine the diffusion coefficient. The total insensitivity of our samples after 3 h at 90°C cannot be explained by monomer out-diffusion alone. The diffusion is not fast enough as indicated by the in-diffusion experiments. We think that the residual thermal radical polymerisation is responsible for the disappearance of monomer in the bulk material.

3.2. Photoinitiator Reaction

The discussion in the previous section excludes the observed reaction of the Cp_2TiCl_2 photoinitiator with moisture. The chemical reaction is given by [14]



The reaction leads to an insensitive product. This results help to understand the depth profiles of in-

diffused samples (Fig. 9). Next to the surface there is an insensitive region due to insensitive photoinitiator according to reaction (13). The depth of this region depends on the residual moisture of the atmosphere mainly during the annealing procedure for 3 h at 90°C .

3.3. Profiles of Photosensitivity

So far we have discussed two different mechanisms influencing the photosensitivity of $\text{Cp}_2\text{TiCl}_2:\text{PMMA}$ samples:

- the concentration of monomer and
- the concentration of photosensitive Cp_2TiCl_2 .

Both components are necessary for the photochemically induced residual polymerisation. Multiplication of both profiles leads to a photosensitivity profile. In the linear region of the recording growth curve, that is for low exposure energies, we have a linear response of our photorefractive material.

$$\Delta n(z) = K \cdot S(z) \cdot I \cdot t. \quad (14)$$

The constant c in (12) is replaced by a photosensitivity profile $S(z)$ and a constant K representing the photochemical reactions radical formation and Δn growth. The recording intensity in (14) is given by (10) and we have to consider

$$\Delta n(z) = K \cdot S(z) \cdot t \cdot I_0 \cdot \exp[-\int \alpha(z) dz]. \quad (15)$$

Thus in the linear region $\Delta n(z)$ is given by folding the photosensitivity profile with the light intensity distribution. An example is illustrated in Fig. 15. The single profiles for the case of in-diffused monomer are shown and the resulting profile according to (13) is plotted as a thick line. This profile is comparable to the experimental results of, e.g., Fig. 9.

For the indiffused MMA samples the monomer profiles towards the bulk material may be described by the complementary error function, $\text{erfc}(z)$. In this

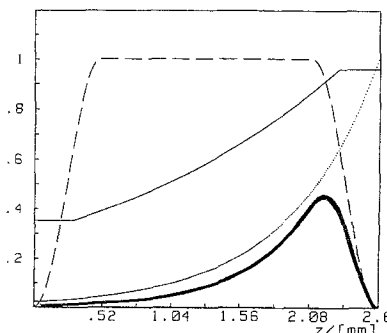


Fig. 15. Superposition of photosensitivity profiles. — Light intensity, — concentration of photoinitiator, ···· monomer concentration, — superposed profile

region $\alpha(z)$ is constant and the monomer profile is identical with the photosensitivity profile $s(z)$. Neglecting the influence of $I(z)$ we can assume $\Delta n(z) \sim s(z)$ as a rough estimate. Measuring $\Delta n(z)$ for different diffusion times one can estimate the diffusion constant for MMA in PMMA for a set of $\Delta n(z)$ profiles. For our diffusion temperature we get $D = (0.014 \pm 0.005) \text{ mm}^2/\text{h}$.

4. Conclusion

A method for measuring profiles in volume phase gratings is described. The monomer concentration is found to be the main source for these profiles. Insensitive samples of PMMA containing a photoinitiator may be sensitized again by MMA in-diffusion.

Using Cp_2TiCl_2 as a photoinitiator for the green laser light leads to additional profiles due to a reaction of Cp_2TiCl_2 with moisture.

The final $\Delta n(z)$ profiles are the product of photosensitivity and the distribution of exposed light throughout the sample.

Acknowledgements. We would like to thank Prof. E. Krätzig for support and discussion and J. Wibbelmann for his help with

sample preparation. Financial support of „Stiftung Volkswagenwerk“ is gratefully acknowledged.

References

1. W.J. Tomlinson, E.A. Chandross: *Adv. Photochem.* **12**, 201 (1980)
2. W.J. Tomlinson, E.A. Chandross, I.P. Kaminov, H.R. Weber, G.D. Amiller: *Appl. Opt.* **15**, 534 (1976)
3. A. Bloom, R.A. Bartolini, H.A. Weakliem: *Opt. Eng.* **17**, 446 (1978)
4. W.S. Colburn, K.A. Haines: *Appl. Opt.* **10**, 1636 (1971)
5. Z.T. Tsai, C.H. Brubaker, Jr., J. Organomet: *Chem.* **166**, 199 (1979)
6. M. Kopietz, M.D. Lechner, D.G. Steinmeier, H. Franke: *Makromol. Chem.* **187**, 2787 (1986)
7. M. Kopietz, J. Marotz, H. Franke, D.G. Steinmeier, M.D. Lechner, E. Krätzig: *Polym. Photochem.* **5**, 109 (1984)
8. J. Marotz: *Appl. Phys.* **B 37**, 181 (1985)
9. J.M. Moran, I.P. Kaminov: *Appl. Opt.* **12**, 1964 (1973)
10. H. Kogelnik: *Bell. Syst. Techn. J.* **48**, 2909 (1969)
11. L. Solymar, D.J. Cooke: *Volume Holography and Volume Gratings* (Academic, London 1981)
12. U. Killat: *Opt. Commun.* **21**, 110 (1977)
13. R. Viewey, D. Braun: *Kunststoff-Handbuch*, Bd. I (Hanser, München 1975)
14. Y.I. Israeli: *Bull. Soc. Chim. France* 837 (1966)